

BARIUM FERRITE MATERIAL SYNTHESIZED ON A SOLAR FURNACE

Paizullakhanov Mukhammade-Sultankhan, Shermatov Javahir, Sabirov Salim

Institute of Materials Science Academy of Sciences of the Republic of Uzbekistan (Uzbekistan, Tashkent)

IJASR 2019

VOLUME 2

ISSUE 3 MAY – JUNE

ISSN: 2581-7876

Abstract – The synthesis process of materials for example ferrous barium oxide in a solar furnace was studied. It was shown that when the $\text{BaCO}_3 + \text{Fe}_2\text{O}_3$ mixtures of concentrated solar radiation are exposed to high ($350\text{W}/\text{cm}^2$) density, barium hexagonal ferrite $4(\text{Fe}_2\text{O}_3)4(\text{FeO})\text{BaFeO}_{3-x}$ is formed and the cubic $\text{Ba}_3\text{Fe}_2\text{O}_{6-x} = 2(\text{BaO})\text{FeOBaFeO}_{3-x}$, tetragonal BaOFeOBaFeO_{3-x} modifications.

Keywords: Magnetic material, solar furnace, structural defects, dielectric constant.

Introduction

To obtain barium ferrite, the initial reagents were used: barium carbonate BaCO_3 iron dioxide Fe_2O_3 . The powders were mixed in the required proportion and were briquetted. Melting of a mixture of iron oxide and barium carbonate on the focal plane of the solar furnace when exposed to a concentrated light flux of $350\text{W}/\text{cm}^2$ density with an exposure to the melting state for 15 minutes. The melts were cooled in air (10^2 degrees / s) and in running water (10^3 degrees/s).

X-ray phase and X-ray diffraction analyzes of the samples under study were carried out on diffractometers DRON-3M ($\text{CuK}\alpha$ radiation). The measurements were carried out at room temperature. The resistivity was measured by the method of current-voltage characteristics and the double-probe method [1]. When conducting electrical measurements used copper contacts deposited by sputtering. The magnetodielectric effect (MD effect, magnetic intensity) was recorded by changing the dielectric constant when the sample was introduced into a magnetic field.

$$\Delta(H)/\epsilon(0) = (\epsilon(H) - \epsilon(0)) / \epsilon(0)$$

where $\epsilon(H)$ and $\epsilon(0)$ are dielectric constant in the magnetic field and without him.

The registration of the magnetodielectric effect was carried out in a constant magnetic field of intensity $H=3.0$ kOe.

Figure 1 shows microscopic photographs of $\text{BaCO}_3 + \text{Fe}_2\text{O}_3$ melts cooled a) in air (10^2 degrees/s) and b) in running water (10^3 degrees/s).

Analysis of microscopic images showed that melts consist of particles of various sizes and shapes. In the case of air cooling, the morphology of the melt corresponds to a fine-grained structure with particle sizes of 1-5 microns, and in the case of cooling in water - 10 - 20 microns.

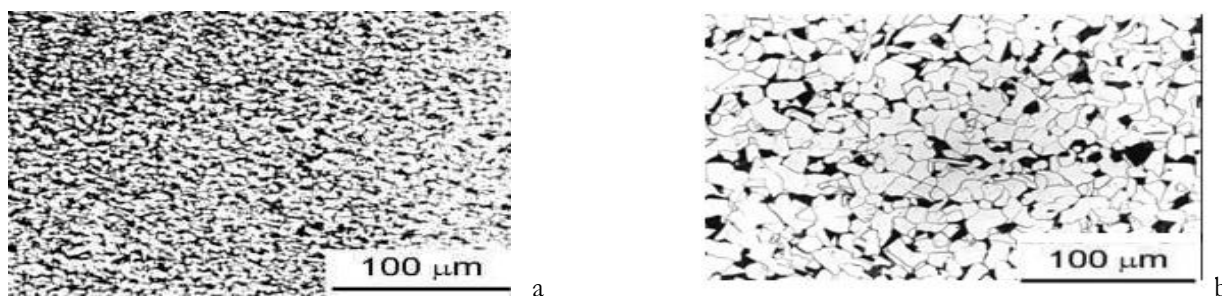


Fig.1. Microscopic images of $\text{BaCO}_3 + \text{Fe}_2\text{O}_3$ melts cooled a) in air (10^2 degrees/s) and b) in running water (10^3 degrees/s)

Figure 2 shows the X-ray diffraction patterns of BaCO₃ + Fe₂O₃ melts cooled a) -n air (10² degrees/s), b) in running water (10³ degrees/s), c) -baked at a temperature T = 1300⁰ C

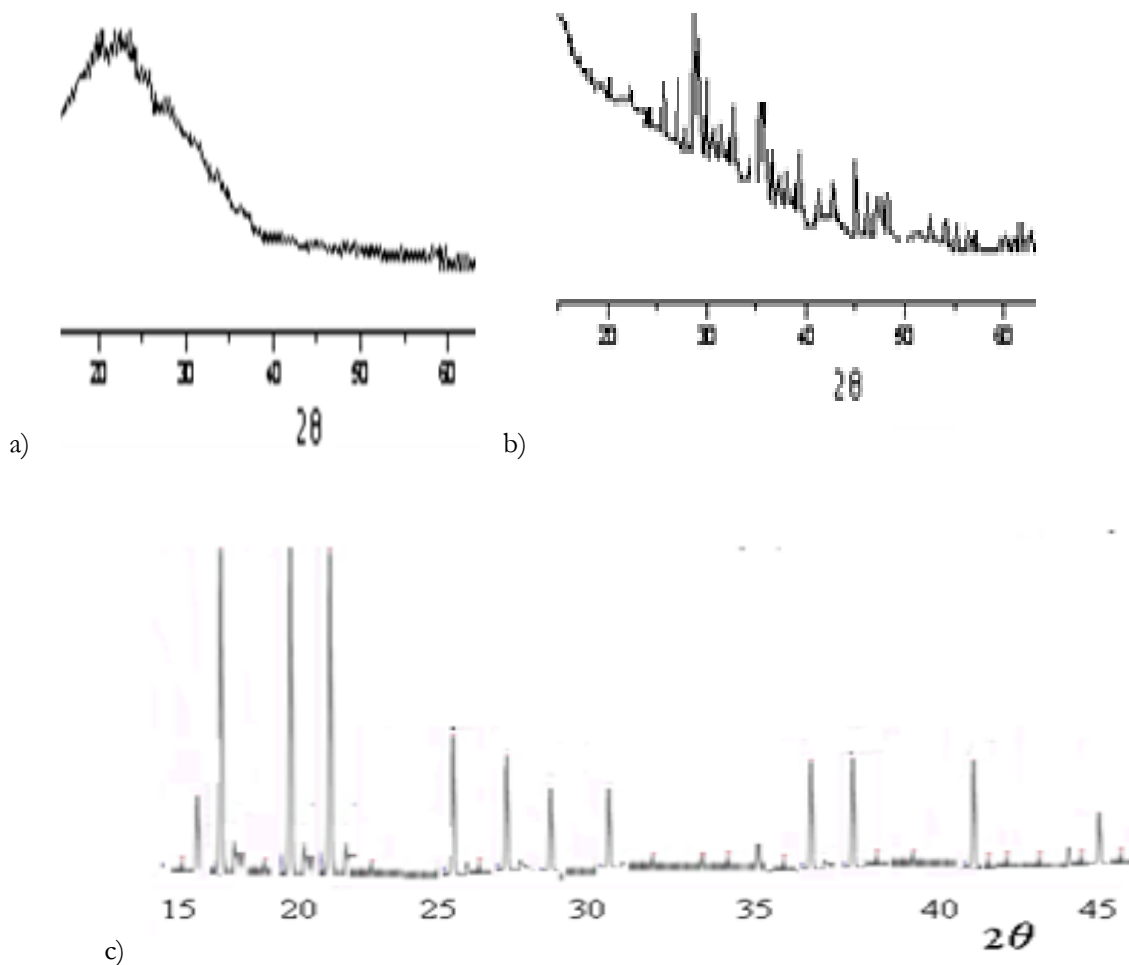


Fig.2. X-ray diffraction patterns of BaCO₃ + Fe₂O₃ melts cooled a) in air (10² degrees / s), b) in running water (10³ degrees / s); c) calcined at a temperature of T = 1300 ° C.

From the analysis of radiographs of BaCO₃ + Fe₂O₃ melts cooled a) - in air (10² degrees/s) and b) in running water (10³ degrees/s) it follows that, depending on the cooling rate, the material can be obtained in varying degrees of amorphism. Quenching in water allows you to fix the amorphous state of matter. While cooling in air on the surface of a water-cooled substrate results in a mixture of amorphous and crystalline phases — a glass-ceramic material.

X-ray diffraction studies showed that the samples calcined at a temperature T = 1300⁰ C were polycrystalline and were a mixture of barium ferrite phases of various modifications — hexagonal ferrous barium oxide 4 (Fe₂O₃) 4 (FeO) BaFeO_{3-x} with lattice parameters a = 5. 86, c = 23. 2 Å, cubic Ba₃Fe₂O_{6-x} = 2 (BaO) FeOBaFeO_{3-x} with the parameter a = 16.79Å, tetragonal BaOFeOBaFeO_{3-x} with the parameters a = 5.98, c = 13.93 Å [1].

Table 1 shows the results of LCR measurements of barium ferrite depending on the type of samples.

Table 1. The results of LCR measurements of barium ferrite

Samples	ε	C, μΦ
quenching in water	22340	920
Slow air cooling	19210	790

Sintered after quenching	14600	600
Solid-phase synthesis in an electric furnace	7450	540

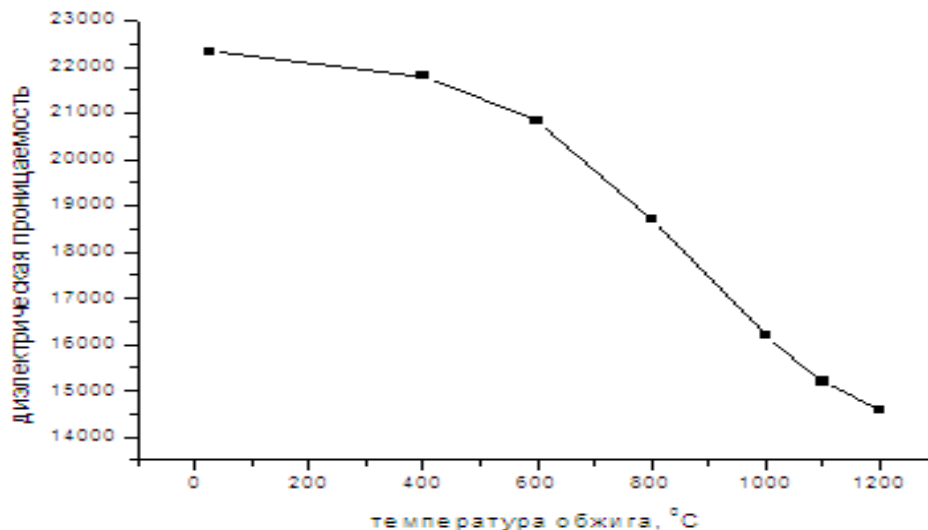


Fig.3. The dependence of the dielectric constant A1-type samples, annealed at different temperatures.

As can be seen from table 1, A-type samples exhibit enhanced dielectric properties compared with B-and C-type samples.

Figure 3 shows the dependence of the dielectric constant of the A1-type of samples annealed at different temperatures.

From Fig. 3 it can be seen that with an increase in the firing temperature, the dielectric constant decreases in comparison with the fused sample. This is due to the fact that when melting on a solar furnace under the influence of high-density concentrated solar radiation, a large number of oxygen vacancy-type structure defects are formed, mainly in the border areas, which cause an increase in the dielectric constant [2-5]. These defects are fired during thermal roasting in air, and a decrease in the dielectric constant of the material is observed.

References

1. Wang J., Neaton J.B., Zheng H. et. al. Epitaxial BiFeO₃ Multiferroic Thin Film Heterostructures// Science.- 2003. Vol. 299. P. 1719-1722.
2. AA Abdurakhmanov, SA Faiziev, RY Akbarov, SK Suleimanov, MK Rumi. Properties of pyroxene glass ceramics, heat treated in the Big Solar Furnace//Applied Solar Energy 45 (1), 45-47
3. MS Paizullakhanov, SA Faiziev, SR Nurmatov, ZZ Synthesis features of barium titanate in the field of concentrated light energy.//Applied Solar Energy 49 (4), 248-250
4. AA Abdurakhmanov, MS Paizullakhanov, Z Akhadov. Synthesis of calcium aluminates on the big solar furnace Applied Solar Energy 48 (2), 129-131
5. RY Akbarov, MS Paizullakhanov. Characteristic Features of the Energy Modes of a Large Solar Furnace with a Capacity of 1000 kW//Applied Solar Energy 54 (2), 99-109